IEEE Access
Multidisciplinary | Rapid Review | Open Access Journal

Received 14 September 2022, accepted 25 September 2022, date of publication 4 October 2022, date of current version 12 October 2022.

Digital Object Identifier 10.1109/ACCESS.2022.3211943

RESEARCH ARTICLE

Performance Analysis of Cooperative Dynamic Framed Slotted-ALOHA With Random Transmit Power Control in A2G Communication Networks

JUNSEUNG LEE[1], (Student Member, IEEE), SEUNGMIN LEE[1], (Student Member, IEEE), SEONG HO CHAE[2], (Member, IEEE), AND HOWON LEE[1], (Senior Member, IEEE)

[1]School of Electronic and Electrical Engineering and IITC, Hankyong National University, Anseong 17579, South Korea
[2]Department of Electronics Engineering, Tech University of Korea, Siheung 15073, South Korea

Corresponding authors: Howon Lee (hwlee@hknu.ac.kr) and Seong Ho Chae (shchae@tukorea.ac.kr)

This work was supported in part by the Institute of Information and Communications Technology Planning and Evaluation (IITP) Grant by the Korean Government [Ministry of Science and ICT (MSIT)] (Development of 3D-NET Core Technology for High-Mobility Vehicular Service, 50%) under Grant 2022-0-00704, and in part by the National Research Foundation of Korea (NRF) Grant by the Korean Government (MSIT) (50%) under Grant 2022R1A2C1010602.

ABSTRACT In this study, we investigate the use of low-altitude unmanned aerial vehicles (UAVs) in air-to-ground (A2G) communication networks, which still have various issues and challenges. In particular, the limited battery power of UAVs render their flight time extremely short. Hence, we present cooperative dynamic framed slotted-ALOHA (CDFS-ALOHA), which is capable of random transmit power control (TPC). When collisions occur, because UAVs can select their retransmit power randomly, their power consumption is reduced and their probability of successful packet transmission is improved owing to a capture effect. In terms of performance metrics, we consider the successful packet transmission probability, UAV power consumption, and network-wide energy efficiency. CDFS-ALOHA with TPC can directly reduce the transmit power consumption of UAVs compared to CDFS-ALOHA without TPC; thus, intra- and intercell interference can be reduced. Consequently, CDFS-ALOHA with TPC can obtain sporadic and intermittent capture effects, thus improving the network-wide energy efficiency without reducing the probability of successful packet transmission in A2G communication networks.

INDEX TERMS Dynamic framed slotted-ALOHA, transmit power control, successful packet transmission probability, power consumption, energy efficiency, air-to-ground (A2G) communication networks.

I. INTRODUCTION

Fifth generation (5G) and beyond 5G (B5G) mobile communications have been investigated and developed to support three usage scenarios: enhanced mobile broadband, ultra-reliable and low-latency communications, and massive machine-type communications [1], [2], [3], [4]. The proliferation of various mobile applications has resulted in an exponential increase in the number of devices and the emergence of diverse devices, and thus many enabling technologies (i.e., multiple-input and multiple-output non-orthogonal multiple-access (MIMO-NOMA) and integrated access and backhaul (IAB) networks) are actively investigated to support these applications [5], [6]. Recently, the utilization of low-altitude unmanned aerial vehicles (UAVs) has increased rapidly owing to their advantages, i.e., providing seamless and secured three-dimensional (3D) wireless connectivity, resolving the problem of shaded areas, reducing the required power consumption for UAV-assisted communications, and supporting flexible ground data acquisition [7], [8], [9], [10], [11], [12], [13], [14]. However, many challenges are to be considered when employing UAVs in wireless communication. In particular, because of the restricted flight time of UAVs owing to their battery limitations, researchers are striving to improve the energy efficiency of UAVs for their use in 5G and B5G air-to-ground (A2G) communication networks.

The associate editor coordinating the review of this manuscript and approving it for publication was Yang Tang.

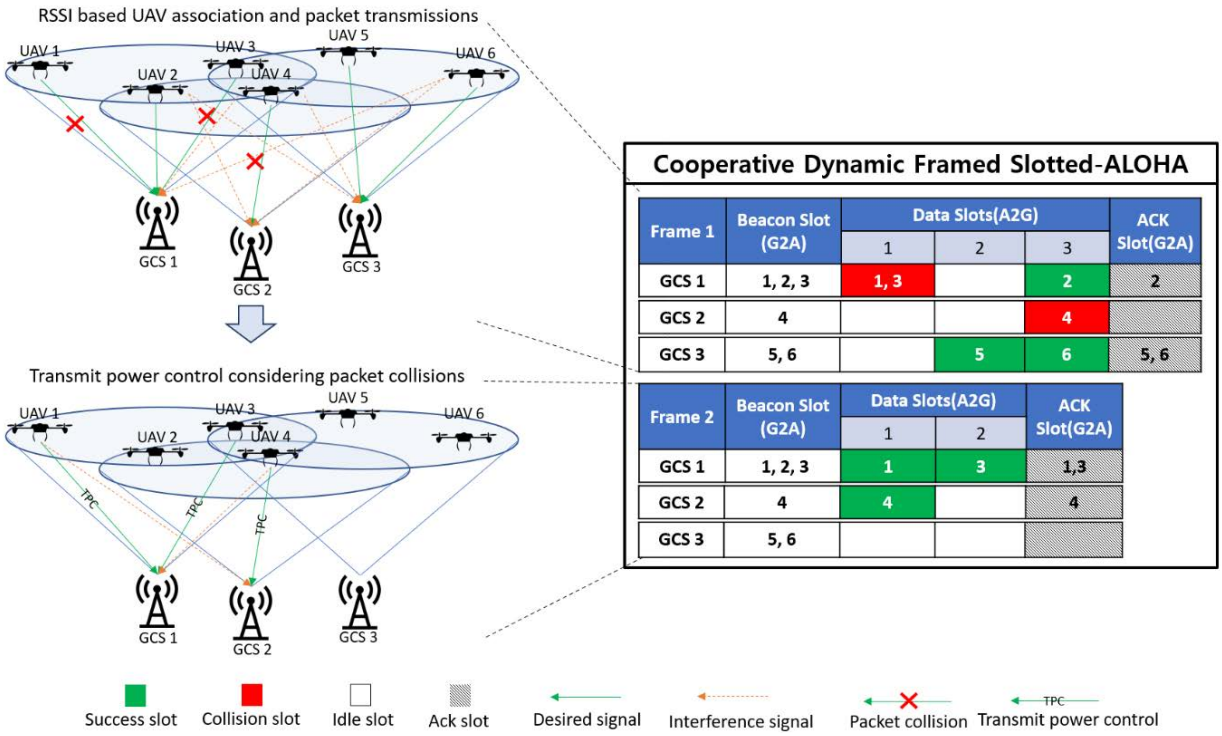

FIGURE 1. System model of cooperative dynamic framed slotted-ALOHA with random transmit power control in uplink multi-cell A2G communication networks.

To achieve this goal, Lee et al. [15] attempted to control the deployment of UAVs and transmit power simultaneously based on multi-agent distributed reinforcement learning to maximize the network-wide energy efficiency in multi-UAV wireless networks. Meanwhile, Fu et al. [16] analyzed the coverage probability and energy efficiency based on the uplink power coefficient and distance between UAVs and a ground control station (GCS). In addition, Lim et al. [17] investigated tethered UAV-base stations (TUAV-BSs), where each TUAV-BS is connected to a building or a ground entity through a tether, which allows the TUAV-BS to be charged continuously through the tether. In that study, the authors proposed a multi-agent reinforcement learning framework to identify the optimal 3D position of TUAV-BSs to maximize the achievable rate. Although these studies attempted to improve the energy efficiency of A2G communication networks through intelligent network deployment and power control, studies that investigate approaches for improving network-wide energy efficiency based on medium access control (MAC) protocols are rare. Therefore, in this study, we analyze the performance of cooperative dynamic framed slotted-ALOHA (CDFS-ALOHA) with random transmit power control (TPC) in A2G communication networks.

The power consumption of UAVs can be categorized into three aspects: standby power consumption, receive power consumption, and transmit power consumption. Among these power consumptions, the transmit power consumption is dominant, but the existing MAC protocols (i.e., framed slotted-ALOHA (FS-ALOHA) and dynamic FS-ALOHA (DFS-ALOHA)) do not control the transmit power of the devices. Therefore, by judiciously adjusting the transmit power of UAVs in A2G communication networks, the power consumption of UAVs can be reduced significantly. Furthermore, FS-ALOHA contains a fixed number of data transmission slots, regardless of whether the packet transmissions are successful. By contrast, DFS-ALOHA adjusts the number of data slots based on the number of active devices in each frame [18], [19]. Because each GCS individually adjusts the number of data slots in DFS-ALOHA, the frame length of the GCSs can be different. Therefore, severe crosslink interference may occur, which results in system performance degradation. In summary, the fixed transmit power and frequent packet retransmissions will result in significant energy wastage when using UAVs in A2G communication networks.

Herein, we present CDFS-ALOHA, which determines the number of data slots in the next frame based on frame-by-frame cooperation between GCSs. Furthermore, we discuss the performance behavior of CDFS-ALOHA with and without TPC in terms of energy efficiency and the successful packet transmission probability based on variations in the horizontal UAV deployment radius and number of UAVs in A2G communication networks.

The remainder of this paper is organized as follows: In Section II, we introduce the elevation angle-dependent probabilistic line-of-sight (LoS) channel model (EPL-CM). In Section III, the random access protocol and power control

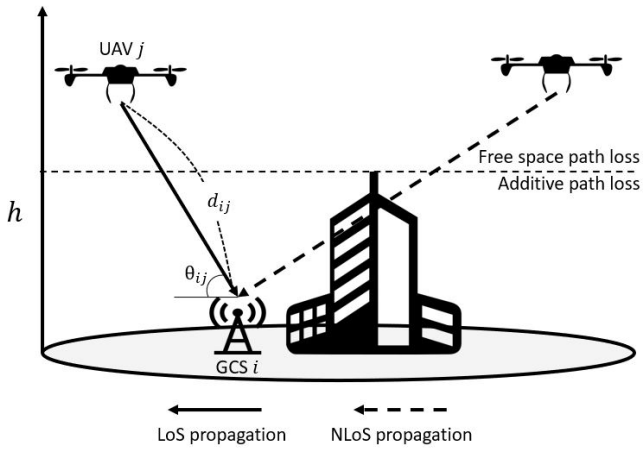

FIGURE 2. Elevation angle-dependent A2G channel model considering LoS and NLoS links.

strategy for uplink multicell A2G communication networks are described. In Section IV, we present and discuss the simulation results of CDFS-ALOHA with and without TPC, separately. Finally, we present the conclusions in Section V.

II. SYSTEM MODEL AND A2G CHANNEL MODEL

In this study, we considered uplink A2G communication networks, as shown in Fig. 1. In a beacon slot, the GCS broadcasts a beacon packet to the UAVs. We assume that each UAV is associated with the GCS that provides the strongest received signal strength indicator (RSSI). After successfully receiving the beacon packet, each UAV attempts to transmit its data packet through one data slot. In this case, several slot situations can occur, such as success, idle, and collision. Subsequently, each GCS informs the UAVs regarding the acknowledgment via the acknowledge (ACK) slot.

To precisely analyze the performance of uplink A2G communication networks, we used an elevation angle-dependent probabilistic A2G channel model that models LoS and non-LoS (NLoS) propagations separately as shown in Fig. 2. In fact, this A2G channel model can be applied to various urban environments, such as suburban, urban, dense urban, and high-rise urban areas [20]. Using approximation with a sigmoid function, Al-Hourani et al. [20] simplified the complicated A2G channel model proposed in [21], thereby utilizing the complex A2G channel model more tractable.

In this A2G channel model, the LoS signal is dominant; therefore, its small-scale fading effect is not significant compared to that of terrestrial mobile networks. Furthermore, by exploiting deployment-specific statistical parameters corresponding to those used in urban environments, the small-scale fading effect could be roughly reflected [15], [22]. The LoS and NLoS probabilities ($P_{ij}^{LoS}(\theta_{ij})$, $P_{ij}^{NLoS}(\theta_{ij})$) between GCS $i \in \mathbb{N}_G$ and UAV $j \in \mathbb{N}_U$ can be calculated as follows:

$$P_{ij}^{LoS}(\theta_{ij}) = \frac{1}{1 + \alpha \times \exp(-\beta \times [\theta_{ij} - \alpha])}, \tag{1}$$

$$P_{ij}^{NLoS}(\theta_{ij}) = 1 - P_{ij}^{LoS}(\theta_{ij}). \tag{2}$$

Here, θ_{ij} is the elevation angle between GCS i and UAV j; α and β are environmental parameters corresponding to deployment in an urban environment. Table 1 shows the statistical parameters for deployments in urban environments such as suburban, urban, dense urban, and high-rise urban areas. In addition, the LoS path loss (L_{ij}^{LoS}) and NLoS path loss (L_{ij}^{NLoS}) between GCS i and UAV j can be represented as follows:

$$L_{ij}^{LoS} = 20\log\left(\frac{4\pi f_c d_{ij}}{c}\right) + \xi^{LoS}, \tag{3}$$

$$L_{ij}^{NLoS} = 20\log\left(\frac{4\pi f_c d_{ij}}{c}\right) + \xi^{NLoS}, \tag{4}$$

where d_{ij} is the distance between GCS i and UAV j; c is the speed of light; f_c is the carrier frequency; ξ^{LoS} and ξ^{NLoS} are the excessive path losses caused by shadowing or scattering, respectively. Using Equations (1)–(4), the average path loss between GCS i and UAV j (L_{ij}^{avg}) can be obtained as follows:

$$L_{ij}^{avg} = P_{ij}^{LoS} \times L_{ij}^{LoS} + P_{ij}^{NLoS} \times L_{ij}^{NLoS}. \tag{5}$$

In addition, based on Equation (5), the SINR between GCS i and UAV j (Γ_{ij}) can be calculated as follows:

$$\Gamma_{ij} = \frac{P_{ij}^{\mathrm{TX}} - L_{ij}^{avg}}{\sigma^2 + \sum_{l=1}^{M} \sum_{k \in \mathbb{N}_l^{\mathrm{IF}}} (P_{ik}^{\mathrm{TX}} - L_{ik}^{avg})}, \tag{6}$$

where P_{ij}^{TX} denotes the transmission power of UAV j to GCS i; σ^2 is the thermal noise power of GCS i; M is the total number of GCSs; $\mathbb{N}_l^{\mathrm{IF}}$ is the set of UAVs that use the same data slot as UAV j in GCS l; $|\mathbb{N}_l^{\mathrm{IF}}|$ is the cardinality of $\mathbb{N}_l^{\mathrm{IF}}$. Failure in packet transmission is assumed when the user's SINR is less than the SINR threshold due to collisions or severe intercell interference.

Since EPL-CM utilizes averaged free-space and additive path losses, it does not directly reflect the small-scale fading effect. So, to compensate for this weakness, EPL-CM introduces statistical parameters (α, β, ξ^{LoS}, ξ^{NLoS}) representing the characteristics of four different urban environmental models (urban, suburban, dense urban, and highrise urban) [22]. If the instantaneous small-scale fading (ISSF) effect is considered, an empirical mean of SINR Γ_{ij}^{avg} can be given by equations (7)–(9), as shown at the bottom of the next page. Here, $L_{ij}^{LoS,ins}$ and $L_{ij}^{NLoS,ins}$ are the instantaneous path losses for the LoS and NLoS channels reflecting the effect of the small-scale fading, respectively. By using Jensen's inequality, we can verify that Γ_{ij} is the upper bound of Γ_{ij}^{avg}. Furthermore, Figs 3a–3c show the performance results considering the instantaneous small-scale fading effect. Specifically, because Γ_{ij} is the upper bound of Γ_{ij}^{avg}, Fig. 3a demonstrates that the successful packet transmission probability of CDFS-ALOHA considering ISSF has slightly smaller than that of CDFS-ALOHA considering EPL-CM. Also, for the same reason, CDFS-ALOHA considering ISSF has more average power consumption than CDFS-ALOHA considering EPL-CM, as shown in Fig. 3b. Similarly, the

TABLE 1. Statistical parameters for urban environmental deployments in A2G channel model [15].

Environment	α	β	ξ^{LoS}[dB]	ξ^{NLoS}[dB]
Suburban	4.8800	0.4290	0.1	21
Urban	9.6117	0.1581	1	20
Dense urban	12.0810	0.1139	1.6	23
Highrise urban	27.2304	0.0797	2.3	34

network-wide energy efficiency of CDFS-ALOHA considering ISSF also becomes less than that of CDFS-ALOHA considering EPL-CM, as shown in Fig. 3c. Consequently, from Figs. 3a–3c, we can find that CDFS-ALOHA considering EPL-CM show very similar performance trends with CDFS-ALOHA considering ISSF, and thus we can conclude that EPL-CM well reflects the practical A2G channel characteristics.

III. CDFS-ALOHA AND TPC STRATEGY

In this study, we consider CDFS-ALOHA, which determines the number of data slots in the next MAC frame via frame-by-frame cooperation between GCSs. As shown in Fig. 1, the frame of CDFS-ALOHA comprises a beacon slot, data slots, and an ACK slot. A detailed description of these slots is provided below:

- **Beacon slot (G2A link)**: Each GCS sends a beacon packet to its associated UAVs. The beacon packet includes the current frame number, the GCS identifier, and the number of data and ACK slots. In addition, the UAV's association is determined using the RSSI value of the beacon packet. The G2A link denotes the ground-to-air communication link.
- **Data slot (A2G link)**: Each UAV selects a data slot to transmit its own packet in each frame. In this study, we assume that packet transmission is successful if the received SINR of the user is greater than the SINR threshold. In this case, we regard the corresponding slot as a "success." In addition, if no UAV sends a packet in the corresponding slot, then the slot is regarded as "idle." Furthermore, if two or more UAVs send packets using the same data slot, we assume that the status of this slot is "collision." However, when a collision occurs, if the SINR of one of the received packets is greater than the SINR threshold, then this packet is considered a successful packet.
- **ACK slot (G2A link)**: The GCS informs the UAVs regarding the acknowledgment of all data slots in every frame. After receiving the ACK packet, UAVs that have successfully transmitted their own packets enter the standby state in the next frame. In addition, UAVs that fail in packet transmission should attempt to send the packet in the next frame.

Assume that GCS i comprises N_i UAVs in cell, and that GCS i assigns $D_i(t)$ data slots based on the number of active UAVs at frame t. Initially, $D_i(t) = N_i(t)$ in CDFS-ALOHA. Because GCS i comprises $N_i^{suc}(t)$ successful UAVs at frame t, $\{N_i(t) - N_i^{suc}(t)\}$ UAVs should attempt to transmit their own packets to GCS i again at frame $t+1$. Before the beginning of frame $t+1$, all GCSs share the number of the next data slots via wired backhaul connections. For instance, GCS i shares the value, $N_i(t) - N_i^{suc}(t)$, with its neighbor GCSs. As a result, the number of data slots at frame $t+1$ can be determined cooperatively and calculated as

$$D_i(t+1) = \max_i (N_i(t) - N_i^{suc}(t)). \tag{10}$$

By determining the number of data slots using Equation (10), crosslink interference (downlink-to-uplink and uplink-to-downlink) can be completely removed in CDFS-ALOHA. In particular, the downlink signal is extremely strong as compared to the uplink signal; therefore, the severity of SINR degradation may be reduced. For example, assume a scenario involving three GCSs and six UAVs, as illustrated in Fig. 1. In the first frame, GCS 1 comprises three UAVs and the highest number of GCSs. Accordingly, in CDFS-ALOHA, the number of data slots is three in the first frame. The UAVs attempt to transmit their packets to the associated GCS using one of the randomly selected data slots. In Fig. 1, the red, green, and white slots represent the slot status of collision, success, and idle, respectively. After completing the first frame, because UAV 2 performed packet transmission successfully, two UAVs remained in GCS 1. Consequently, based on Equation (10), the maximum number of associated UAVs will be two; thus, the number of data slots will be two in the second frame. Based on the abovementioned process, the frames are repeated until one of the termination conditions

$$\Gamma_{ij}^{avg} = \left[P_{ij}^{LoS} \times \mathbb{E}\left(\frac{P_{ij}^{\mathrm{TX}} / L_{ij}^{LoS,ins}}{\sigma^2 + \sum_{l=1}^{M} \sum_{k \in \mathbb{N}_l^{\mathrm{IF}}} P_{ik}^{\mathrm{RX}}} \right) + P_{ij}^{NLoS} \times \mathbb{E}\left(\frac{P_{ij}^{\mathrm{TX}} / L_{ij}^{NLoS,ins}}{\sigma^2 + \sum_{l=1}^{M} \sum_{k \in \mathbb{N}_l^{\mathrm{IF}}} P_{ik}^{\mathrm{RX}}} \right) \right] \tag{7}$$

$$\leq \left[P_{ij}^{LoS} \times \left(\frac{P_{ij}^{\mathrm{TX}} / L_{ij}^{LoS}}{\sigma^2 + \sum_{l=1}^{M} \sum_{k \in \mathbb{N}_l^{\mathrm{IF}}} P_{ik}^{\mathrm{RX}}} \right) + P_{ij}^{NLoS} \times \left(\frac{P_{ij}^{\mathrm{TX}} / L_{ij}^{NLoS}}{\sigma^2 + \sum_{l=1}^{M} \sum_{k \in \mathbb{N}_l^{\mathrm{IF}}} P_{ik}^{\mathrm{RX}}} \right) \right] \tag{8}$$

$$\leq \frac{P_{ij}^{\mathrm{TX}} / L_{ij}^{\mathrm{avg}}}{\sigma^2 + \sum_{l=1}^{M} \sum_{k \in \mathbb{N}_l^{\mathrm{IF}}} P_{ik}^{\mathrm{RX}}} = \Gamma_{ij}. \tag{9}$$

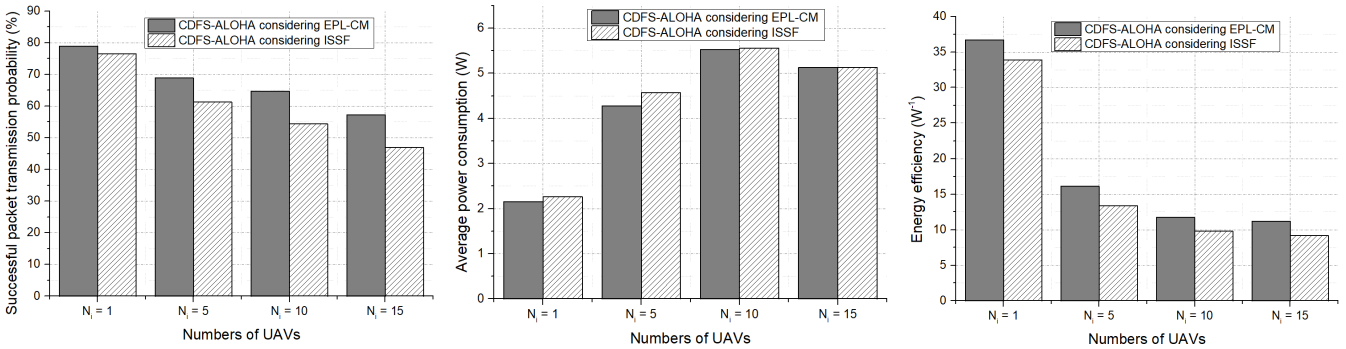

(a) Successful packet transmission probability vs. number of UAVs

(b) Average power consumption vs. number of UAVs

(c) Energy efficiency vs. number of UAVs

FIGURE 3. Successful packet transmission probability, average power consumption, and energy efficiency vs. number of UAVs for CDFS-ALOHA considering EPL-CM and CDFS-ALOHA considering ISSF.

(TCs) is satisfied. The detailed TCs of CDFS-ALOHA are as follows:

- **TC1:** The packets of all UAVs are successfully transmitted under the packet retransmission opportunities and within the packet expiration time.
- **TC2:** All UAVs transmit packets up to the maximum number of retransmissions before reaching the packet expiration time; beyond that, the UAVs can no longer transmit their packets.
- **TC3:** The packet expires regardless of whether it is successfully transmitted or the maximum number of retransmissions is reached.

In the mandatory mode, CDFS-ALOHA employs fixed power for both transmission and retransmission. Alternatively, the TPC method can be applied in packet retransmissions to simultaneously reduce power consumption and improve the successful packet transmission probability. We refer to this mode herein as the TPC mode. In the retransmissions, we set the transmit power to be random in the TPC mode. This power control can reduce the power consumption of the UAVs directly and improve the successful packet transmission probability via a capture effect.

IV. SIMULATION RESULTS

A. SIMULATION ENVIRONMENTS

In this study, we considered the average successful packet transmission probability, power consumption of UAVs, and network-wide energy efficiency of UAVs. Here, UAVs are randomly distributed within the horizontal UAV deployment radius. First, the average successful packet transmission probability at frame t ($P^{suc}(t)$) can be represented as follows:

$$P^{suc}(t) = \frac{1}{N}\sum_{i}^{M}\sum_{j}^{N_i}\left(\frac{R_{ij}^{suc}(t)}{R_{ij}^{suc}(t)+R_{ij}^{col}(t)}\right), \tag{11}$$

where M, N, and N_i are the total number of GCSs, UAVs, and UAVs associated with GCS i, respectively. In addition, $R_{ij}^{suc}(t)$ and $R_{ij}^{col}(t)$ represent the number of success and collision slots at frame t, respectively. The success of the packet transmission is determined by the SINR threshold, which is the minimum SINR value to support the lowest modulation and coding scheme level [23]. That is, if the SINR of a certain UAV that sent a packet to the associated GCS exceeds the SINR threshold, then the corresponding slot used by this UAV to transmit the packet is considered successful. In this paper, we set the SINR threshold to 0 dB for A2G communication networks [8], [24]. In addition, the average power consumption of the UAV at frame t ($E^{PC}(t)$) can be represented by Equations (12), as shown at the bottom of the next page, where, $R_{ij}^{beacon}(t)$ and $R_{ij}^{\mathrm{ACK}}(t)$ are the number of beacon and ACK slots, respectively, and $R_{ij}^{wait}(t)$ is the number of idle slots that no UAV attempts to transmit. Additionally, P_{ij}^{TX} and P_{ij}^{RX} are the power consumed for packet transmission and reception, respectively. P_{ij}^{wait} denotes the power consumed in the standby mode. Table 2 shows the detailed simulation parameters used to obtain the simulation results in terms of the successful packet transmission probability, UAV power consumption, and network-wide energy efficiency.

B. RESULTS AND DISCUSSION

1) NECESSITY FOR ADJUSTMENT OF THE NUMBER OF SLOTS: FS-ALOHA VS. CDFS-ALOHA

Fig. 4 shows the network-wide energy efficiency vs. the number of UAVs of FS-ALOHA with and without TPC, and CDFS-ALOHA with and without TPC under the suburban environment with horizontal UAV deployment radius of 1000 m. The proposed CDFS-ALOHA determines the number of data transmission slots in the next frame based on frame-by-frame cooperation between GCSs. However, FS-ALOHA always contains a fixed number of data transmission slots regardless of whether the packet transmissions are successful. As a result, the network-wide energy efficiency of the proposed CDFS-ALOHA is better in all cases, as shown in Fig. 4. In addition, when applying TPC, the consumed energy of UAVs can be reduced in retransmissions, and thus both protocols can obtain performance gains in terms of energy efficiency.

TABLE 2. Simulation parameters.

Parameter	Value
Carrier frequency	3 [GHz]
Number of cells	7
GCS spacing	300 [m]
Number of beacon slots	2
Number of data slots	Variable
Number of ACK slots	1
Slot length	50 [ms]
Number of iterations	1000
UAV's altitude	120∼150 [m]
Transmit power consumption	1 [W] (No TPC), 0.1∼1 [W] (TPC)
Receive power consumption	0.2 [W]
WAIT power consumption	0.1 [W]
SINR outage threshold	0 [dB]
Maximum number of retransmissions	3
Packet expiration time	2000 [ms]

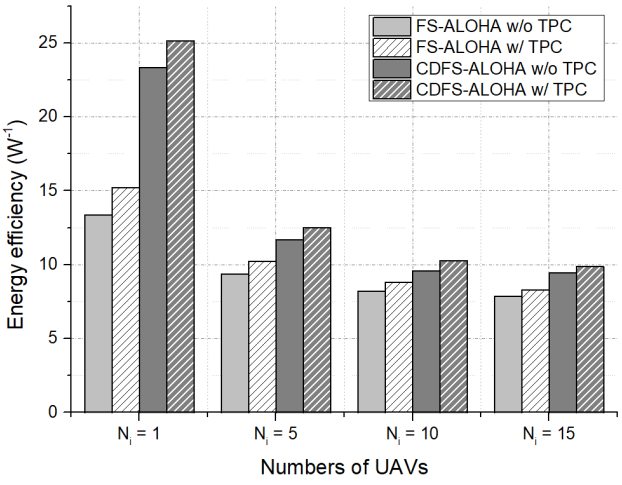

FIGURE 4. Energy efficiency vs. number of UAVs for FS-ALOHA and CDFS-ALOHA with TPC, and FS-ALOHA and CDFS-ALOHA without TPC.

2) NECESSITY FOR TRANSMIT POWER CONTROL: W/TPC VS. W/O TPC

Fig. 5, 6, and 7 are the results for the suburban environment. First, Fig. 5 shows the successful packet transmission probability vs. the horizontal UAV deployment radius of CDFS-ALOHA with and without TPC according to variations in the number of UAVs. From this figure, it can be seen that CDFS-ALOHA without and with TPC have similar performance results in terms of the successful packet transmission probability. Since we assume that CDFS-ALOHA without TPC always transmits its packets with the maximum transmit power, TPC can help reduce intra- and intercell interferences as well as yield the capture effect, and therefore it can prevent reducing the successful packet transmission probability. When $N_i = 1$, the probability of successful packet transmission decreases as the horizontal UAV deployment radius increases, as shown in Fig. 5. If exactly one UAV is associated with each GCS, then no intracell interference occurs. This implies that the signal attenuation increases exponentially based on the distance between the GCS and the associated UAV, particularly from 100 m to 200 m. Furthermore, as the horizontal UAV deployment radius increases from 200 m to 1000 m, the number of UAVs associated with each GCS occasionally exceeds one. In this case, more collisions may occur in cells comprising two or more associated UAVs, resulting in a lower successful packet transmission probability. By contrast, when $N_i = 5$, 10, and 15, increasing the horizontal UAV deployment radius may result in less dense network environments, thereby resulting in an increase in the successful packet transmission probability until a radius of 700 m. Also, when the horizontal UAV deployment radius exceeds 700 m, the effect of the desired signal attenuation based on the distance between the GCS and UAVs becomes more dominant as compared to the effects of the intra- and intercell interferences. Thus, the probability of successful packet transmission decreases gradually. Furthermore, when $N_i = 15$, there exist a number of nodes where the desired signal attenuation is relatively severe compared to the attenuation of the interference signals as the distance increases from 100 m to 200 m, so that the successful packet transmission probability is temporarily reduced.

Fig. 6 shows the average power consumption of the UAVs vs. the horizontal UAV deployment radius of CDFS-ALOHA with and without TPC when the number of UAVs in each cell is 1, 5, 10, and 15 in a suburban environment. When the

$$E^{PC}(t) = \frac{1}{N}\sum_{i}^{M}\sum_{j}^{N_i}\left\{\left(R_{ij}^{beacon}(t)+R_{ij}^{\mathrm{ACK}}(t)\right)\times P_{ij}^{\mathrm{RX}}+\left(R_{ij}^{suc}(t)+R_{ij}^{col}(t)\right)\times P_{ij}^{\mathrm{TX}}+R_{ij}^{wait}(t)\times P_{ij}^{wait}\right\}. \tag{12}$$

$$\eta(t) = \sum_{i}^{M}\sum_{j}^{N_i}\left[\frac{R_{ij}^{suc}(t)}{\left(R_{ij}^{suc}(t)+R_{ij}^{col}(t)\right)\times\left\{\left(R_{ij}^{beacon}(t)+R_{ij}^{\mathrm{ACK}}(t)\right)\times P_{ij}^{\mathrm{RX}}+\left(R_{ij}^{suc}(t)+R_{ij}^{col}(t)\right)\times P_{ij}^{\mathrm{TX}}+R_{ij}^{wait}(t)\times P_{ij}^{wait}\right\}}\right]. \tag{13}$$

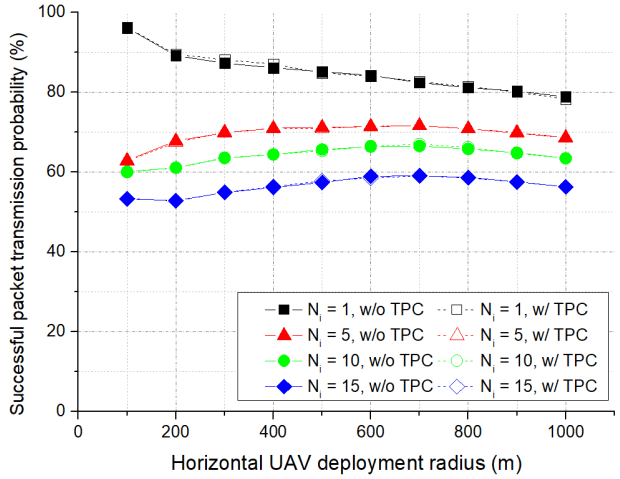

FIGURE 5. Successful packet transmission probability vs. horizontal UAV deployment radius for CDFS-ALOHA with TPC and CDFS-ALOHA without TPC.

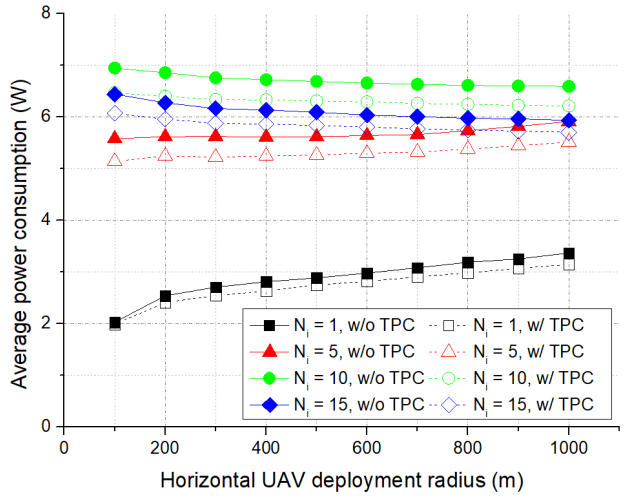

FIGURE 6. Average power consumption vs. horizontal UAV deployment radius for CDFS-ALOHA with TPC and CDFS-ALOHA without TPC.

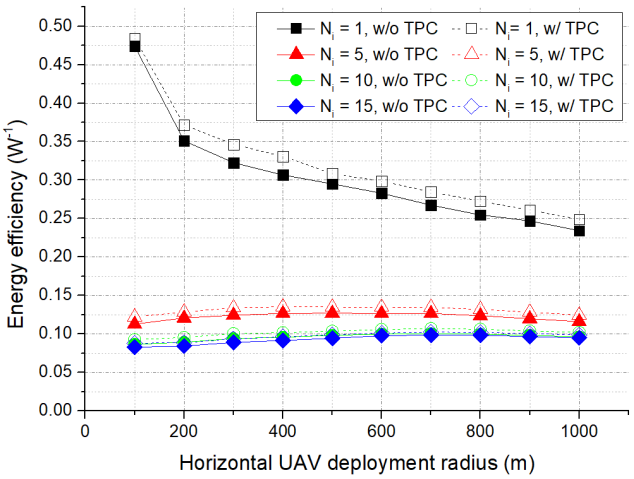

FIGURE 7. Energy efficiency vs. horizontal UAV deployment radius for CDFS-ALOHA with TPC and CDFS-ALOHA without TPC.

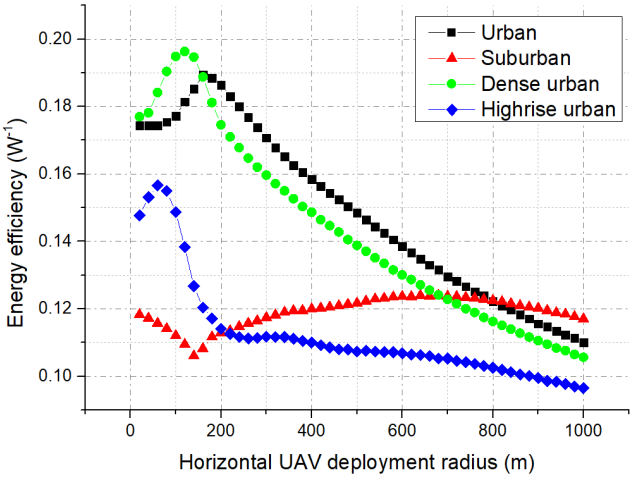

FIGURE 8. Energy efficiency vs. horizontal UAV deployment radius for CDFS-ALOHA in different environments with TPC.

numbers of UAVs become 10 and 15, increasing the horizontal UAV deployment radius results in biased UAV deployment. Thus, the frame length in CDFS-ALOHA becomes larger than that of DFS-ALOHA, and therefore it reduces the undesired retransmissions of unidentified UAVs. It may cause a reduction in UAVs' power consumption. Also, as shown in Fig. 6, since CDFS-ALOHA without TPC always sends its packet with the maximum transmit power, CDFS-ALOHA with TPC can reduce the power consumption significantly compared to CDFS-ALOHA without TPC.

Fig. 7 shows the network-wide energy efficiency obtained using Equation (13), as shown at the bottom of the previous page vs. the horizontal UAV deployment radius of CDFS-ALOHA with and without TPC when the numbers of UAVs in each cell are 1, 5, 10, and 15 in the suburban environment. The results show that CDFS-ALOHA with TPC achieved a higher $\eta(t)$ compared to CDFS-ALOHA without TPC. Even though the UAVs' retransmit power might become weaker, the capture effect can compensate for this problem, thereby allowing a high network-wide energy efficiency gain to be achieved.

3) VARIATIONS IN ENVIRONMENTAL DEPLOYMENTS

Fig. 8 shows the performance of CDFS-ALOHA with TPC based on the various environmental deployments proposed by International Telecommunication Union-Radio communication sector (ITU-R) (i.e., suburban, urban, dense urban, and high-rise urban areas). The characteristics of each environmental deployment are represented as statistical parameters (α, β, ξ^{LoS}, and ξ^{NLoS}), as summarized in Table 1. As shown in Fig. 8, in the case of a suburban environment, the energy efficiency of CDFS-ALOHA gradually decreases up to 160 m as the increase in the LoS path loss dominates the attenuation of the interfering signal. By contrast, the energy efficiency steadily increases in the range of 160 m and beyond, where the effect of path loss is insignificant. In the

urban, dense urban, and high-rise urban environments, the energy efficiency increases rapidly up to 160, 120, and 60 m, respectively, owing to the degree of UAV scattering. After the peak point, the energy efficiency decreases significantly owing to the severe path loss and interference.

V. CONCLUSION

In this paper, we presented CDFS-ALOHA with TPC and compared its performance with that of CDFS-ALOHA without TPC in terms of the successful packet transmission probability, UAV power consumption, and network-wide energy efficiency. The results showed that CDFS-ALOHA can significantly reduce the power consumption of UAVs significantly by exploiting random TPC. In the CDFS-ALOHA with TPC, even though its transmit power reduced, it indicated a decrease in intra- and intercell interferences. Furthermore, owing to sporadic and intermittent capture effects, the probability of successful packet transmission was almost never reduced. In addition, we demonstrated that an increase in the horizontal UAV deployment radius might result in less dense network conditions, which might consequently increase the successful packet transmission probability. Our simulation results showed that the horizontal UAV deployment radius is a critical parameter that affects the performance in terms of network-wide energy efficiency.

REFERENCES

[1] *6G: The Next Hyper-Connected Experience for All*, Samsung Research, Bengaluru, Karnataka, Jul. 2020.
[2] F. Tariq, M. R. A. Khandaker, K.-K. Wong, M. A. Imran, M. Bennis, and M. Debbah, "A speculative study on 6G," *IEEE Wireless Commun.*, vol. 27, no. 4, pp. 118–125, Aug. 2020.
[3] H. Yu, H. Lee, and H. Jeon, "What is 5G? Emerging 5G mobile services and network requirements," *Sustainability*, vol. 9, pp. 1–22, Oct. 2017.
[4] A. Slalmi, H. Chaibi, A. Chehri, R. Saadane, and G. Jeon, "Toward 6G: Understanding network requirements and key performance indicators," *Trans. Emerg. Telecommun. Technol.*, vol. 32, no. 3, p. e4201, Dec. 2020.
[5] L. Xiao, Y. Li, C. Dai, H. Dai, and H. V. Poor, "Reinforcement learning-based NOMA power allocation in the presence of smart jamming," *IEEE Trans. Veh. Technol.*, vol. 67, no. 4, pp. 3377–3389, Apr. 2018.
[6] W. Lei, Y. Ye, and M. Xiao, "Deep reinforcement learning-based spectrum allocation in integrated access and backhaul networks," *IEEE Trans. Cogn. Commun. Netw.*, vol. 6, no. 3, pp. 970–979, Sep. 2020.
[7] Y. Zeng, R. Zhang, and T. J. Lim, "Wireless communications with unmanned aerial vehicles: Opportunities and challenges," *IEEE Commun. Mag.*, vol. 54, no. 5, pp. 36–42, May 2016.
[8] R. Amer, W. Saad, and N. Marchetti, "Mobility in the sky: Performance and mobility analysis for cellular-connected UAVs," *IEEE Trans. Commun.*, vol. 68, no. 5, pp. 3229–3246, May 2020.
[9] B. Li, Z. Fei, and Y. Zhang, "UAV communications for 5G and beyond: Recent advances and future trends," *IEEE Internet Things J.*, vol. 6, no. 2, pp. 2241–2263, Apr. 2019.
[10] A. Masaracchia, Y. Li, K. K. Nguyen, C. Yin, S. R. Khosravirad, D. B. D. Costa, and T. Q. Duong, "UAV-enabled ultra-reliable low-latency communications for 6G: A comprehensive survey," *IEEE Access*, vol. 9, pp. 137338–137352, 2021.
[11] S. Lim, S. H. Chae, and H. Lee, "RE-ORA: Residual energy-aware online random access for improving the lifetime of slotted ALOHA-based swarming drone networks," *IEEE Access*, vol. 9, pp. 45504–45511, 2021.
[12] L. Xiao, Y. Ding, J. Huang, S. Liu, Y. Tang, and H. Dai, "UAV anti-jamming video transmissions with QoE guarantee: A reinforcement learning-based approach," *IEEE Trans. Commun.*, vol. 69, no. 9, pp. 5933–5947, Sep. 2021.
[13] S. Lee, S. Lim, S. H. Chae, B. C. Jung, C. Y. Park, and H. Lee, "Optimal frequency reuse and power control in multi-UAV wireless networks: Hierarchical multi-agent reinforcement learning perspective," *IEEE Access*, vol. 10, pp. 39555–39565, 2022.
[14] A. Masaracchia, L. D. Nguyen, T. Q. Duong, C. Yin, O. A. Dobre, and E. Garcia-Palacios, "Energy-efficient and throughput fair resource allocation for TS-NOMA UAV-assisted communications," *IEEE Trans. Commun.*, vol. 68, no. 11, pp. 7156–7169, Nov. 2020.
[15] S. Lee, H. Yu, and H. Lee, "Multi-agent Q-learning based multi-UAV wireless networks for maximizing energy efficiency: Deployment and power control strategy design," *IEEE Internet Things J.*, vol. 9, no. 9, pp. 6442–6534, May 2022.
[16] X. Fu, T. Ding, M. Kadoch, and M. Cheriet, "Uplink performance analysis of UAV cellular communications with power control," in *Proc. Int. Wireless Commun. Mobile Comput. (IWCMC)*, Jun. 2020, pp. 676–679.
[17] S. Lim, H. Yu, and H. Lee, "Optimal tethered-UAV deployment in A2G communication networks: Multi-agent Q-learning approach," *IEEE Internet Things J.*, vol. 9, no. 19, pp. 18539–18549, Oct. 2022, doi: 10.1109/JIOT.2022.3161260.
[18] D. K. Klair, K.-W. Chin, and R. Raad, "A survey and tutorial of RFID anti-collision protocols," *IEEE Commun. Surveys Tuts.*, vol. 12, no. 3, pp. 400–421, 3rd Quart., 2010.
[19] J. Liu, H. Lee, and H. Jin, "Multichannel S-ALOHA-enabled autonomous self-healing in industrial IoT networks," *IEEE Trans. Ind. Informat.*, vol. 18, no. 12, pp. 8576–8585, Dec. 2022, doi: 10.1109/TII.2022.3149908.
[20] A. Al-Hourani, S. Kandeepan, and S. Lardner, "Optimal LAP altitude for maximum coverage," *IEEE Wireless Commun. Lett.*, vol. 3, no. 6, pp. 569–572, Dec. 2014.
[21] *Propagation Data and Prediction Methods for the Design of Terrestrial Broadband Millimetric Radio Access Systems*, document Rec. P.1410-2, ITU-R, 2003.
[22] Y. Zeng, Q. Wu, and R. Zhang, "Accessing from the sky: A tutorial on UAV communications for 5G and beyond," *Proc. IEEE*, vol. 107, no. 12, pp. 2327–2375, Dec. 2019.
[23] T. Kwon et al., "Design and implementation of a simulator based on a cross-layer protocol between MAC and PHY layers in a WiBro compatible IEEE 802.16e OFDMA system," *IEEE Commun. Mag.*, vol. 43, no. 12, pp. 136–146, Dec. 2005.
[24] Y. Gao, L. Xiao, F. Wu, D. Yang, and Z. Sun, "Cellular-connected UAV trajectory design with connectivity constraint: A deep reinforcement learning approach," *IEEE Trans. Green Commun. Netw.*, vol. 5, no. 3, pp. 1369–1380, Sep. 2021.

JUNSEUNG LEE (Student Member, IEEE) received the B.S. degree from the School of Electronic and Electrical Engineering, Hankyong National University, Anseong, South Korea, in 2022. His current research interests include B5G/6G wireless communications, ultra-dense distributed networks, reinforcement learning for UAV networks, unsupervised learning for wireless communication networks, and the Internet of Things.

SEUNGMIN LEE (Student Member, IEEE) received the B.S. degree from the School of Electronic and Electrical Engineering, Hankyong National University, Anseong, South Korea, in 2021. His current research interests include B5G/6G wireless communications, ultra-dense distributed networks, reinforcement learning for UAV networks, unsupervised learning for wireless communication networks, and the Internet of Things. He was a recipient of the Best Paper Award at KICS Winter Conference, in 2020, and the Best Paper Award at the KICS Summer Conference, in 2022.

SEONG HO CHAE (Member, IEEE) received the B.S. degree from the School of Electronic and Electrical Engineering, Sungkyunkwan University, Suwon, South Korea, in 2010, and the M.S. and Ph.D. degrees from the School of Electrical Engineering, Korea Advanced Institute of Science and Technology (KAIST), Daejeon, South Korea, in 2012 and 2016, respectively. He was a Postdoctoral Research Fellow with KAIST, in 2016. He was a Senior Researcher with the Agency for Defense Development, from 2016 to 2018, where he was involved in research and development for military communication system and frequency management software. He is currently an Assistant Professor with the Tech University of Korea. His research interests include edge computing and caching, UAV communications, and the Internet of Things (IoT).

HOWON LEE (Senior Member, IEEE) received the B.S., M.S., and Ph.D. degrees in electrical and computer engineering from the Korea Advanced Institute of Science and Technology (KAIST), Daejeon, South Korea, in 2003, 2005, and 2009, respectively. From 2009 to 2012, he was a Senior Research Staff/a Team Leader at the Knowledge Convergence Team, KAIST Institute for Information Technology Convergence (KI-ITC). Since 2012, he has been with the School of Electronic and Electrical Engineering, Institute for IT Convergence (IITC), Hankyong National University (HKNU), Anseong, South Korea. He has also experienced as a Visiting Scholar with the University of California San Dieo (UCSD), La Jolla, CA, USA, in 2018. His current research interests include B5G/6G wireless communications, ultra-dense distributed networks, in-network computations for 3D images, cross-layer radio resource management, reinforcement learning for UAV networks, unsupervised learning for wireless communication networks, and the Internet of Things.

He was the recipient of the Joint Conference on Communications and Information (JCCI) 2006 Best Paper Award and the Bronze Prize at Intel Student Paper Contest, in 2006. He was also a recipient of the Telecommunications Technology Association (TTA) Paper Contest Encouragement Award, in 2011; the Best Paper Award at the Korean Institute of Communications and Information Sciences (KICS) Summer Conference, in 2015; the Best Paper Award at the KICS Fall Conference, in 2015; the Honorable Achievement Award from the 5G Forum Korea, in 2016; the Best Paper Award at the KICS Summer Conference, in 2017 and 2018; and the Best Paper Award at the KICS Winter Conference, in 2018 and 2020. He received the Minister's Commendation by the Ministry of Science and ICT, in 2017.